International Journal of
Sensor Networks and Data Communications

Richardson et al., Sensor Netw Data Commun 2016, 5:1
DOI: 10.4172/2090-4886.1000137

Research Article Open Access

Light-Weight Energy Consumption Model and Evaluation for Wireless Sensor Networks

Andrew Richardson, Jordan Rendall and Yongjun Lai*

Mechanical and Materials Engineering, Queens University, Kingston, Ontario, K7L 3N6, Canada

Abstract

Wireless sensor networks are comprised of low power devices with fixed energy stores. They often require long term operation for successful deployment so it is important to efficiently manage and track their energy usage. To effectively accomplish this across distributed networks requires methods which have low energy cost with minimal error. In this paper we present a straightforward model for energy consumption in wireless sensor networks which is light-weight and accurate. The model has been applied to a wireless sensor network developed by the Queen's University MEMs lab and is evaluated with a custom testbed. Through testing, the model is exposed to realistic disturbances of communication loss, battery effects and variable voltage supplies. It was shown that with 99% packet reception rates in the network, the model accurately estimates end node energy consumption with less than 5% error. These results were demonstrated across varying data rates, battery supply capacities, and runtimes up to full network lifetime.

Keywords: Wireless sensor networks; Energy model; Energy consumption

Introduction

Wireless sensor networks (WSNs) have shown promise in support of a wide range of applications from wildlife telemetry tags [1] to structural health monitoring of civil structures [2]. Additionally, WSNs have shown prospective use in industrial applications such as industrial machine monitoring where they can potentially reduce system cost and provide flexible testing platforms [3]. WSN are commonly comprised of battery powered nodes which require extended deployment durations to be successful. Because of this, lowering power consumption of WSNs is of major importance.

One method to lower WSN power consumption this is through the monitoring of node energy. Through this monitoring, researchers have shown possible reductions in WSN energy usage with techniques such as component-aware dynamic voltage scaling [4] and duty-cycle reconfigurable sensor electronics [5]. Monitoring node energy consumption across a distrusted WSN adds additional challenges. It requires a method which is able to wirelessly track energy usage with high accuracy while imposing minimal additional energy consumption on the system.

There has been some energy aware WSNs methods proposed in research that have shown promise. These methods include energy aware frame work with a focus on fault tolerance [6], a protocol for energy-aware LED lighting system control [7] and a stochastic model for a gradient based routing protocol [8]. The testing of these methods has been primarily through simulation, presenting the need for experimental validation of an energy consumption model to be performed.

Here we present a light-weight, energy consumption model and test its accuracy with experimental measurements. To remain light-weight, the model uses end node source voltage measurements, which are commonly taken and transmitted in many WSNs, and timing information taken by mains powered gateways. Through testing with a WSN developed by the Queen's University MEMs Lab, (referred to as QML-WSN), the model is shown to accurately represent the end node energy consumption while being exposed to communication issues, battery effects such as rate capacity and recovery, and variable supply voltages over extended test durations.

The rest of this paper is presented in the subsequent format. Section of testbed and experimental methods details the experimental setup used and further describes QML-WSN. WSN Energy Characterization section explains the energy characterization steps required for implementing the model for a WSN, while Energy Model section describes how the model functions and the initial tuning required. Model testing details the testing performed to validate the model and later important results are discussed. Last section summarizes the main conclusions of the work.

Testbed and Experimental Methods

To evaluate the energy consumption model, a testbed for controlled WSN operation with simultaneous measurement of end node energy consumption was created. The testbed consists of two groups of components: the WSN under test and the measurement equipment (Figure 1). Time stamped current measurements and collected input data for the model allows the characterization of a WSN's energy usage, tuning of the model, and evaluation of the model's performance.

The QML-WSN is a star network designed for industrial monitoring which consists of one gateway and end nodes that communicate wirelessly over 2.4 GHz band. The gateway schedules communication timeslots and data requests for the end nodes, while the end nodes periodically collect and transmit data to the gateway. A controlled DC power supply or batteries can be used as the end node power supply allowing flexibility in testing. The gateway is connected to the computer over an Ethernet switch for user control of the WSN and the storage of WSN collected data into a MySQL database, which is used as input to the model. Only one end node is used during the testing demonstrated

***Corresponding author:** Yongjun Lai, Mechanical and Materials Engineering, Queens University, Kingston, Ontario, K7L 3N6, Canada, Tel: 16135336535; E-mail: lai@queensu.ca

Received February 03, 2016; **Accepted** February 25, 2016; **Published** March 03, 2016

Citation: Richardson A, Rendall J, Lai Y (2016) Light-Weight Energy Consumption Model and Evaluation for Wireless Sensor Networks. Sensor Netw Data Commun 5: 137. doi:10.4172/2090-4886.1000137

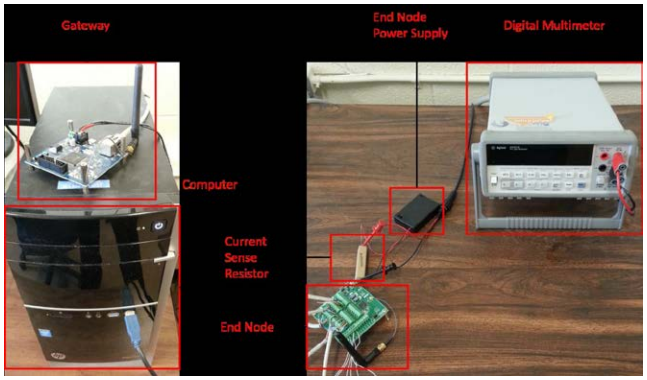

Figure 1: Experimental test bed for measuring WSN end node energy consumption during operation.

in the paper. To emulate the application requirements of QML-WSN, 5 STMicroelectronics LIS3DHTR accelerometers and 3 US Sensor USP11491 thermistors were connected to the end node sensor ports for the collection of acceleration and temperature data.

The measurement equipment is comprised of: one Key sight 34401A digital multi meter, a 10 Ω 25 W current sense resistor, and a computer. To measure end node current with minimal added loading, the digital multi meter measures the voltage drop across the current sense resistor which is in series between the end node power supply and the end node. The digital multi meter is controlled by the computer over GPIB through Lab VIEW script to store and capture voltage measurements at 226 Hz with +/- 0.1 μV resolution, or 1 μA of end node current.

For each test the desired data rate was set on the gateway, the end node was connected to the power supply and current measurements from the digital multi meter were started as the WSN operation began. A test was ended after either a set period of time elapsed or the end node supply voltage dropped below the functional range. During all testing, QML-WSN was operated with normal application behavior while current was measured from the digital multi meter.

QML-WSN's end node function is to remain primarily in a low energy usage sleep mode and periodically transition into a high energy usage active mode at the allocated timeslot. When in active mode, the end node first transmits a 'wake up' message to the gateway to ensure proper timing and then receives a data request message from the gateway. The end node samples its supply voltage, collects acceleration and temperature data from its sensors and transmits this data back to gateway in a 'data' message. A typical 'data' message is 1424 bits, including headers. The end node then transitions back to sleep mode. Through control of the gateway time slot scheduling the data rate can be set for the end node.

The time stamped current data measured during end node operation was processed in MATLAB to provide behavior specific end node energy consumption over a test's duration. The behaviors were isolated by identifying the transitions between sleep and active modes through derivative peak detection of the current measurements. The current measurements for each active and sleep period were integrated, resulting in end node energy consumption for each active and sleep period. The resulting measured end node energy information is used to characterization the WSN energy consumption. Additionally, since the measured energy information is time synchronized with the MySQL database, which is used as an input to the model, it can provide experimental measurements to directly compare with the model.

WSN Energy Characterization

The initial step to applying an energy consumption model is to characterize the WSN nodes energy usage [9]. This involves measuring the node energy usages for behaviors of interest to system operation across the working supply voltage range. Researchers have demonstrated highly detailed WSN profiling [9,10], but for QML-WSN, the behaviors of interest can be more plainly modeled as fixed sleep periods and fixed active period.

Using the testbed and techniques described in the above section, QML-WSN's current draw was measured for supply voltages of 5 V - 2.5 V from a controlled DC power supply. Measurements for each supply voltage were taken over 18 h - 24 h tests and the currents observed for sleep and active periods over the testing duration were each averaged. The resulting measured average currents, per supply voltage, for active and sleep behaviors can be seen in Figures 2a and 2b respectively. It can be seen that the active current is approximately three orders of magnitude larger than the sleep current, as the active periods are where we expect the majority of end node energy consumption. Linear fits have been applied to the measured data to form piecewise functions for active and sleep current dependent on supply voltage. Looking more closely at Figure 2, sections 1 of both the active and sleep current are the result of voltage regulation across the external TPS62740 converter [11]. At the supply range of 3.5 V - 2.5 V, the system is regulated by internal voltage converters of the MCU [12]. This results in linear relationships governed by the internal converters seen in active current section 2 and sleep current section 3. There is also a transitional period between converters for sleep current shown in section 2. Proper system operation does not occur below 2.5 V supply voltage resulting in sleep current spiking (sleep current section 4 in Figure 2b), but this is not included for the summarizing equations or for the model. The piecewise equations 1 and 2 are the result of profiling QML-WSN, providing linear voltage-current relationships for the end node behaviors which are necessary to the proposed energy consumption model.

$$I_{Active}(V_S) = \begin{cases} -2.6912V + 27.508, & V \geq 3.5 \\ 1.2597V + 14.157, & V < 3.5 \end{cases} \quad (1)$$

$$I_{Sleep}(V_S) = \begin{cases} -0.0011V + 0.0103, & V \geq 3.567 \\ -0.0536V + 0.1985, & 3.567 < V \geq 3.25 \\ -0.0029V + 0.0324, & 3.25 < V \geq 2.5 \end{cases} \quad (2)$$

Energy Model

The energy model leverages the known voltage-current relationships gained from WSN profiling along with measured node supply voltages and timing information, collected by the gateway, to estimate energy usage with a minimal computational load required from end nodes. These terms are used to provide energy consumed for each period of node behavior, which are summed. The general model equation is given in (3) where the measured supply voltage V_i is used with the voltage-current relationships $I(V_i)$ to approximate the average current of node periods, while the timing information Δt_i estimates the period durations and E_{sum} is the summation of consumed energy.

$$E_{sum} = \sum_{i=0}^{i=number\ of\ periods} I(V_i)\Delta t_i \quad (3)$$

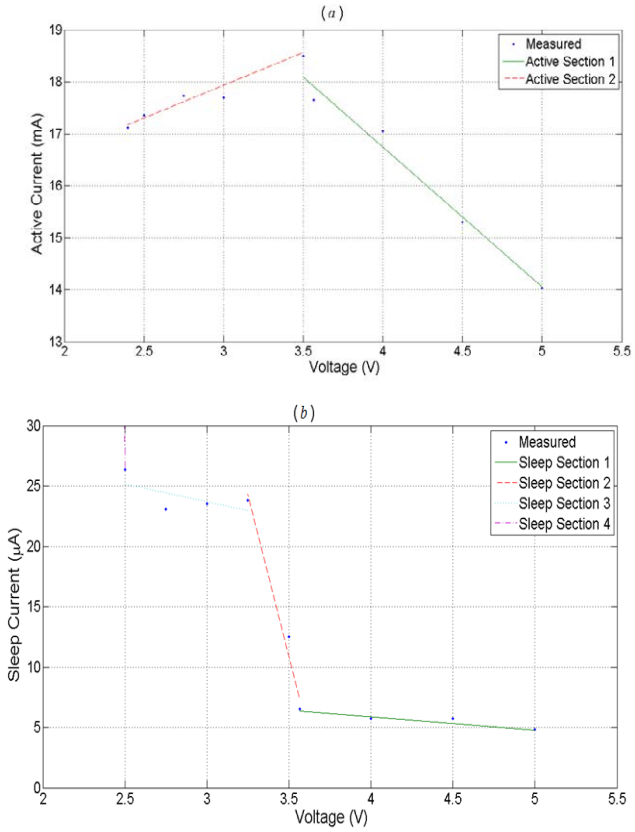

Figure 2: Energy characterization results of end node (a) active and (b) sleep behaviours.

The generic model is modified to allow a minimal computational load required rom nodes. Node information is only sent during node active periods while timing is tracked by the gateway around the active communication intervals, resulting in equation (4).

$$E_{sum} = \sum_{i=0}^{i=number\ of\ periods} I_{Active}(V_i)(t_{data_i} - t_{wake_i}) + I_{Sleep}(V_i)(t_{wake_{i+1}} - t_{data_i}) \quad (4)$$

Where $I_{Active}(V_i)$ and $I_{Sleep}(V_i)$ are the voltage-current relationships for active and sleep node behavior respectively, t_{wake_i} is the time the node 'wakeup' message is receive by the gateway while t_{data_i} is the time the node 'data' message is receive by the gateway, and Vi is the supply voltage measured by the node during the active period. The number of active periods is used for indexing because information collected by the node is only sent during active periods. Using this method, the active periods are directly tracked while the sleep periods occur in the duration between active periods. For calculation of the sleep period current, the supply voltage sampled during the previous active period is used which should show minimal change.

Model development

The model was then applied to a controlled experimental scenario of QML-WSN while true node energy usage was measured from the digital millimeter. Using the test bed with node supply voltage fixed at 3.567 V from a DC power supply, a single node with 11.8 bps data rate was run for 24 hours with no packet losses. The resulting running energy summations plotted against testing time can be seen in Figure 3a, where the model and measured energy summations appear as constant linear energy consumption rates. The model's slope appears lower than that of the measured slope by a constant value, causing an underestimate of node energy consumption. This suggests the underestimate is attributable to a small consistent error in energy calculations of each end node period. It was found that by calculating the weighted mean of the distribution for active period durations over the test, the measured active period duration was 609.8 ms while the modeled was 518.3 ms. This would lead to a 15% underestimate in the models end node active energy from the measured. The timing difference in the model can be attributed to a short portion of the end node active period occurring before the wakeup message is transmitted and after the data message is received by the gateway. This underestimate of active duration can be corrected by computing the difference between the weighted means and adding this calculated correction factor constant to each active period duration in the model, while also shifting the sleep durations. The resulting model is plotted as 'model correction factor' in Figure 3a, where the model and measured energy summations align much more closely.

The model's performance with and without the correction factor can be better seen in Figure 3b, which displays the error in modeled energy summation from the measured results. The error without the correction follows a linear trend with a slope of approximately 1.40 $\times 10^{-2}$ mA, which is expected from the slope difference of energy summation previously observed. It results in a final error of 3.291×10^{-1} mAh or a 14.48% error over the 24 hr test duration. For the model with the correction factor, the error stays very close to zero and is reflective of the close alignment to the measured energy summation. It results in a final error of 1.2×10^{-2} mAh or a 0.528% error over the 24 hr test duration.

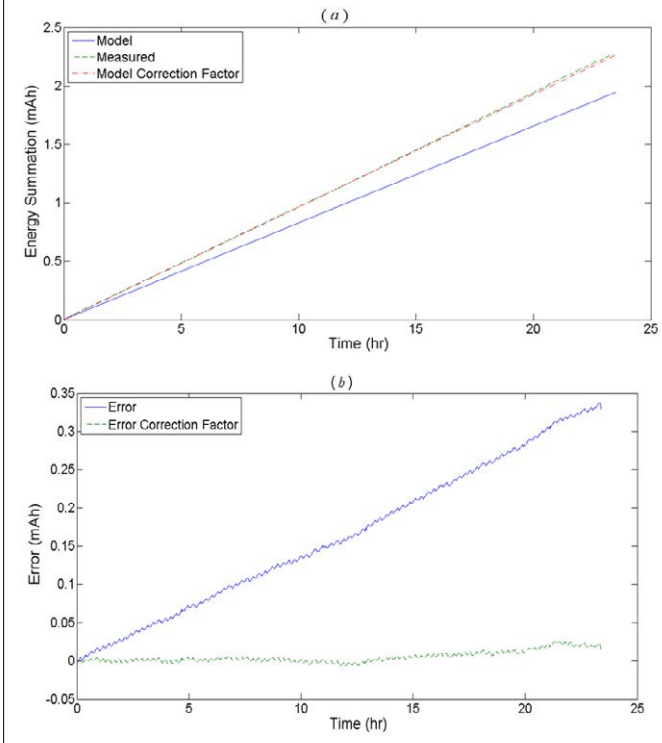

Figure 3: End node measured and modeled energy summations with and without correction in a. Error between measured and modeled energy summations with and without correction factor in b.

The model thus demonstrates it is able to effectively predict the energy consumption of the node within 15% error without the correction factor and this is improved to less than 1% error when including the correction factor. The correction factor will remain constant for QML-WSN since we expect the active period timing to be unchanged. During further use of the model with QML-WSN, the correction factor calculated from this test will be applied.

Model Testing

The proposed energy consumption model has demonstrated the ability to accurately predict node energy under controlled experimental conditions, but this is not always the case with real world WSNs. In WSN deployments nodes can experience communication issues, battery effects such as rate capacity and recovery, and variable supply voltages throughout their lifetime. Two trials were undertaken using the testbed to better examine the impact of these factors on the model and its accuracy. The parameters of each trial are summarized in Table 1 and described in detail below.

In the first trial, the node's data rate was increased to 282.8 bps, the power source was changed to low capacity alkaline batteries, and the node was run until the batteries were fully depleted achieving network lifetime. Network lifetime was deemed to be reached when sustained proper end node function no longer occurred. The increased data rate and low capacity batteries were chosen to accelerate the battery depletion and reduce the testing time required while still achieving full network lifetime. This allowed three tests under the same conditions to be performed. Three Energizer A76 alkaline button batteries in series were used as the power source which has a rated capacity of 153 mAh at a discharge rate of 191 μA [13].

In the second trial, the power source was changed to standard capacity alkaline batteries; the batteries were only partially depleted by fixing the testing length to one week due to time constraints. Two tests were performed with differing data rates of 282.8 bps and 11.8 bps. This trial better reflects realistic application power sources and the associated battery effects, submits the energy consumption model to longer duration testing, and explores the impact of data rates on the model. Three Duracell Procell PC1500 AA alkaline batteries in series were used as the end node power source, which have a rated capacity of 3280 mAh at a discharge rate of 5 mA [14].

Low capacity battery full depletion

For trial 1, three separate tests were conducted under the described experimental conditions. Figure 4a displays the modeled energy summation for each test, and Figure 4b displays the measured energy summation. From Figure 4a, it can be observed that the modeled energy summations of the three tests consist of closely matching linear trends that deviate in slope throughout the tests runtime. The gradual deviations in slope are likely due to end node current draw changing as supply voltage drops from 4.44 V - 2.5 V with battery depletion over the test runtime, as dictated by the profiled voltage-current relationship. Additionally, there is variation between the tests' network lifetime durations and their final modeled energy which ranged from 64.5 h - 75.2 h and 114 mAh - 135.8 mAh respectively. These differences are clarified when looking at the tests' measured energy summations in Figure 4b. It can be observed that the final measured energy for all tests is notably closer, ranging from 129.5 mAh - 136.4 mAh with differing energy consumption rates leading to the variations in test network lifetimes. The final measured energy is still lower than the rated 153 mAh specified by the battery manufacture; this could be attributed to the rate capacity effect from discharging well above the listed rate of 191 μA.

From the measured energy summations in Figure 4b, linear trends similar to the modeled energy are evident but with significantly more variation throughout each of the tests. The variations appear to be due to regions of high energy consumption, between 15 h - 25 h for all three tests and between 0 h - 2.5 h for test 1. It should be noted that communication issues between the end node and gateway were observed during testing around these regions. For each of the three tests the measured energy is higher than the modeled energy, indicating that the model is underestimating the end node energy consumption. The high energy consumption regions are not apparent in the modeled energy summation, suggesting they are introducing error into the model and may be causing an underestimate of end node energy consumption.

Standard capacity battery partial depletion

In trial 2, two separate tests were performed under the experimental conditions previously described. Test 1 used a data rate of 282.8 bps and tests 2 used 11.8 bps. The results of test 1 and 2 are presented in Figures 5a and 5b respectively, displaying the measured and modeled energy summations for each of the tests. Over the 167 h test duration,

Trial number-test number	Data rate	End node power supply	Test duration
1-1	282.8 bps	3x Energizer A76	Full battery depletion
1-2	282.8 bps	3x Energizer A77	Full battery depletion
1-3	282.8 bps	3x Energizer A78	Full battery depletion
2-1	282.8 bps	3x Duracell PC1500	1 week
2-2	11.8 bps		

Table 1: Summary of parameters for each trail and test.

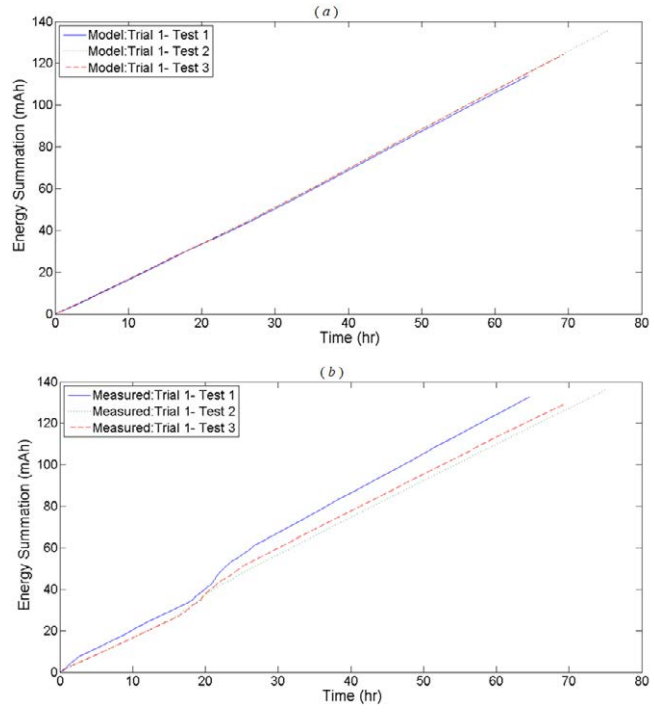

Figure 4: Modeled energy summation results for Trail 1 tests 1-3 in a, and measured energy summation result in b.

the final measured and modeled energy summations for test 1 were 284.2 mAh and 260.4 mAh respectively, while for test 2 they were 11.89 mAh and 11.4 mAh. The difference in final energy between tests 1 and 2 is due to end node data rate. In test 2 the data rate is 24 times lower than the data rate used in test 1.

The modeled energy summations appear to follow similar linear trends to those seen in trial 1with less slope deviations. The steadier slopes may be attributed to more stable supply voltages over the testing duration caused by a lower depletion of the overall battery capacity. The test 1 supply voltage changed from 4.71 V - 4.34 V while test 2 remained even more stable, only changing from 4.68 V - 4.66 V. In the measured energy summations of both tests, multiple regions of high energy usage were again observed. These same trends are observed in both tests of differing data rates, suggesting the model error apply evenly across data rates. The longer test duration with higher data rate of test 1 allowed the observation of a periodic like nature of the high energy usage regions at approximately: 70 h, 90 h, 115 h, 135 h, 160 h (Figure 5a). Also in Figure 5a, the model and measured energy summations appear to intersect at 70 h suggesting there may be competing factors in the energy model for over and undercompensation.

Discussion

To better discern the effects observed during testing and the overall accuracy of the proposed model, the error between the measured and modeled energy summations has been calculated for both trials. The errors for trial 1 test 1-3 and trial 2 tests 1 are displayed in Figure 6a. The error for trial 2 test 2 is plotted in Figure 7a, due to the lower magnitude of energy usage compared to the previous tests. Increases in error can be seen for all tests which coincide closely in time with the high energy usage regions previously observed in the measured

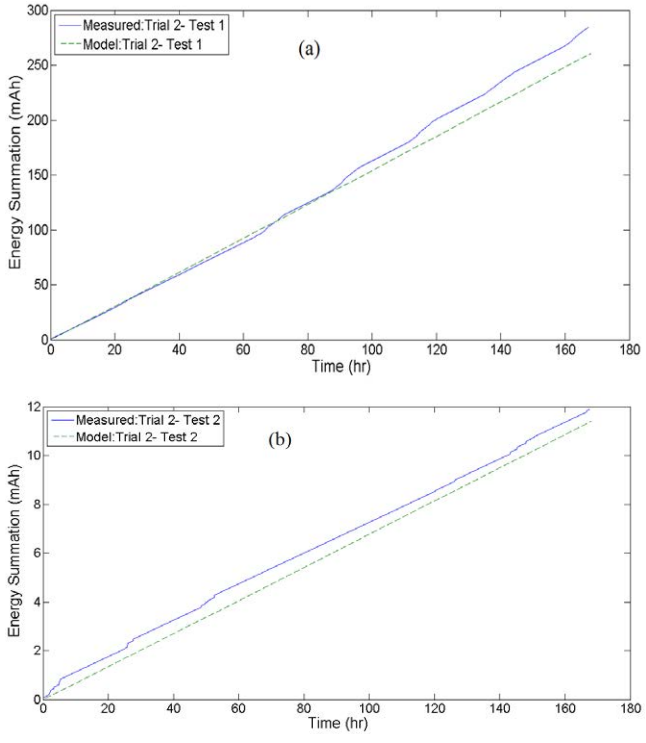

Figure 5: Trial 2 resulting measured and modeled energy summations for test 1, a, and test 2, b.

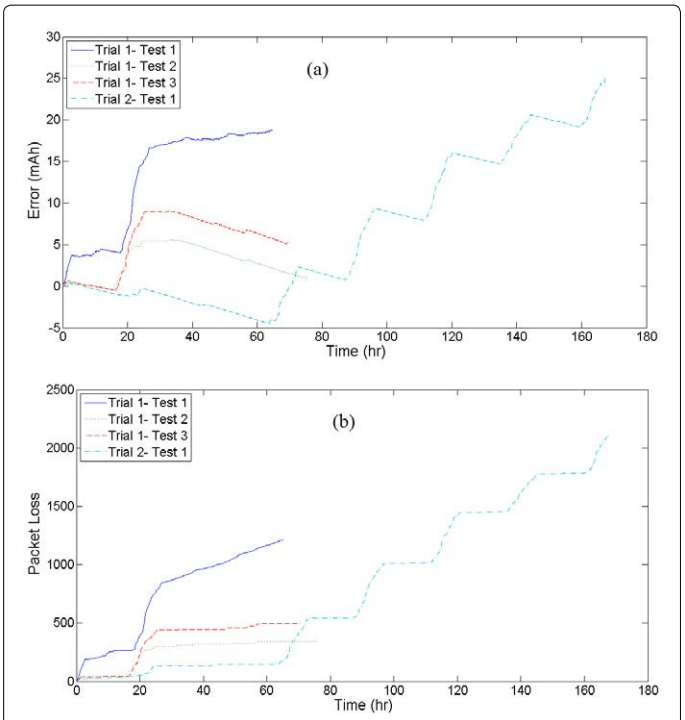

Figure 6: Error between modeled and measured energy summations of trial 1 tests 1-3 and trial 2 test 1 in a and each tests' packet loss in b.

energy summations. The increases appear to be the main source of error introduced into the model and thus require further investigation into their cause.

Packet loss

End node communication interruptions were observed during testing near the high energy usage regions. To clarify the communication interruptions, the packet loss for each test is examined. The cumulative packet loss for trial 1 tests 1-3 and trial 2 tests 1 are shown in Figure 6b, while trial 2 test 2 packet losses is shown in Figure 7b. It can be observed for all tests that regions of high packet loss occur in the same time intervals as every large increase in error. Additionally, little to no packet loss can be observed in the duration between the jumps in error, with the exception of trail 1 test 1 which shows consistent packet losses and corresponding building error. Error introduced by packet loss can be explained by the presented model's reliance on proper communication to account for end node active period energy usage. When proper communication is not received by the gateway, the model estimates the end node to be in the low energy usage sleep mode. This causes the potential for the model to miss high energy usage periods where the node does not successfully communicate with the gateway. Few instances of packet loss without missed active periods can be seen, such as trial 2 test 2 at 80 h in Figure 7, but the majority appear to coincide with missed active periods. The periodic nature of the packet loss observed in Figure 6b for trial 2 test 1 and the high density of the packet loss regions for all tests suggests that packet loss is the main error introduced into the model.

Model overcompensation

A smaller source of error in the model can be observed in Figures 6a and 7a as regions with negative slope in the error plots, which represent overcompensation of energy consumption by the model.

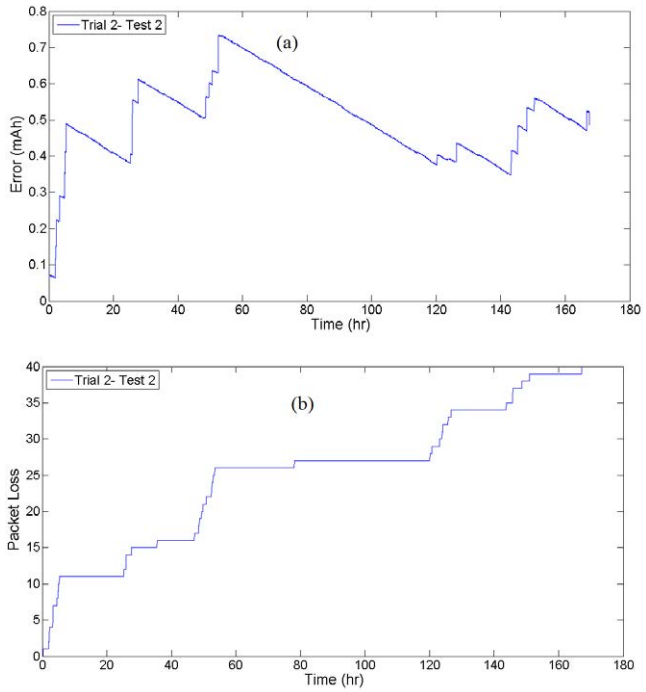

Figure 7: Error between modeled and measured energy summations of trial 2 test 2 in (a) and the test's packet loss in (b).

Trial number - test number	Data rate	Final error (%)	Packet reception rate (%)
1-1	282.8 bps	14.12	97.4
1-2		0.469	99.36
1-3		4.107	99.00
2-1		8.386	98.25
2-2	11.8 bps	4.089	99.21

Table 2: Summary of test accuracy.

The overcompensation appears to occur during regions where packet loss remains stable, as seen in Figure 6b and Figure 7b. As the change in error is gradual, it suggests that it is the result of small miscalculations of energy in each end node period. It can be seen that the overcompensation appears constant for trial 2 test 1, 2 in Figures 6a and 7a, while it appears to change over the duration of trial 1 tests 2, 3. The change in slope can be noted in Figure 6a trial 1 tests 2, 3 as the slope of the error becomes near zero from 25 h - 35 h, which corresponds to source voltages between 3.75 V - 3.55 V for both tests. This suggests that source voltage influences this overcompensation, as it varies significantly more over the duration of the trail 1 tests than the trial 2 tests and it is used in the calculation of each end node period's energy consumption. The cause of the overcompensation could be attributed to an inaccuracy sampling the end node source voltage or misalignment in the current-voltage relationship creating during the energy characterizing. Both of these issues could be improved with calibration of the end node voltage sampling and more detailed energy characterizing. Ultimately, the overcompensation of node energy consumption shown is a minor source of error in the model compared to that caused by the communication issues.

Model accuracy

The overall accuracy of the model can be clarified by examining the final error in each test as a percentage of final measured energy. Table 2 summarizes the final errors and includes each test's packet reception rate. Examining Table 2, the model is seen across all tests to accurately predict energy consumption within 15% error for packet reception rates of 97.4% or greater. The model's accuracy was shown to increase for packet reception rates of 99% or greater, predicting energy consumption with 5% or less error. As packet reception rates of 99% have been feasibly demonstrated in WSN applications [15], it suggests that the model presented could predict energy consumption with 5% or less error in WSN applications. The overall accuracy of the model has been demonstrated to be high with consistency across: testing duration, network lifetime, data rates, battery depletion, and voltage supply capacity.

Conclusion

The focus of this paper is to demonstrate an energy consumption model for WSN nodes that is accurate and light-weight. The model was implemented using a WSN developed by the Queen's University MEMs Lab, QML-WSN. This model is useful for tracking the energy usage throughout a distributed WSN, estimating the realistic network lifetime of a WSN deployment, and enabling energy aware networking protocols. The model was demonstrated and validated through controlled testing while exposing QML-WSN to communication issues, battery effects such as rate capacity and recovery, and variable supply voltages throughout the network lifetime.

To accurately evaluate the model a testbed has been created and detailed. QML-WSN's energy consumption was first characterized and the model was implemented on the platform. QML- WSN was tested under a range of conditions to ensure the model's performance. Two trails were undertaken with differing data rates, battery supply capacities, runtimes up to full battery depletion and network lifetime.

The model's performance was shown to be heavily influenced by packet loss. Despite this, the model still achieved high accuracy with errors lower than 5% for packet reception over 99%. These results were repeated for a range of battery capacities, data rates, network lifetime, and battery depletion. Additionally, a minor source of error of end node energy overcompensation was shown and could be reduced with a more detailed WSN energy characterizing. This model shows promise for a wide range of WSNs that have high packet reception rates. Further work of interest to this model is additional testing with an installed WSN in application environment and added compensation into the model for the error introduced by packet loss.

References

1. Toledo S (2015) Evaluating batteries for advanced wildlife telemetry tags. IET Wirel Sens Syst 5: 235-242.
2. Chintalapudi K, Fu T, Paek J, Kothari N, Rangwala S, et al. (2006) Monitoring civil structures with a wireless sensor network. IEEE Internet Comput 10: 26-34.
3. Hou L, Bergmann NW (2012) Novel industrial wireless sensor networks for machine condition monitoring and fault diagnosis. IEEE Trans Instrum Meas 61: 2787-2798.
4. Hoermann LB, Glatz PM, Steger C, Weiss R (2011) Energy efficient supply of wsn nodes using component-aware dynamic voltage scaling. Wireless conference sustainable wireless technologies (European wireless), Austria.
5. Lutz K, Konig A (2010) Minimizing power consumption in wireless sensor networks by duty cycled reconfigurable sensor electronics. 8th Workshop on Intelligent Solutions in Embedded Systems, Crete.
6. Mitra S, De Sarkar A (2014) Energy aware fault tolerant framework in wireless sensor network. Applications and innovations in mobile computing, Kolkata.
7. Huynh TP, Tan YK, Tseng KJ (2011) Energy-aware wireless sensor network with ambient intelligence for smart LED lighting system control. 37th Annual Conference of the IEEE Industrial Electronics Society, Melbourne.

8. Migabo ME, Djouani K, Kurien AM, Olwal TO (2015) A stochastic energy consumption model for wireless sensor networks using GBR techniques. AFRICON, Addis Ababa.
9. Raghunathan V, Schurgers C, Park SPS, Srivastava MB (2002) Energy aware wireless micro sensor networks. IEEE Signal Process Mag 19: 40-50.
10. Antonopoulos C, Prayati A, Stoyanova T, Koulamas C, Papadopoulos G (2009) Experimental evaluation of WSN platform power consumption. IEEE International symposium on parallel and distributed processing, Rome.
11. Texas instruments (2014) TPS6274x 360nA I Q step down converter for low power applications.
12. Atmel Corporation (2014) ATmega256/128/64RFRS microcontroller with low power 2.4GHz transceiver.
13. Energizer (2015) Energizer A76 Alkaline battery.
14. Duracell (2015) Dyracell ID1500 alkaline manganese dioxide battery.
15. Geng D, Zhao Z, Fang Z, Xuan Y, Zhao J (2010) GRDT: group based reliable data transport in wireless body area sensor networks. IET International conference on wireless sensor network, Beijing.